Web: www.witpress.com Email witpress@witpress.com
Paper from: *Design and Nature*, CA Brebbia, L Sucharov & P Pascola (Editors).
ISBN 1-85312-901-1

Experimental evidences for chaotic dynamics in the roar of the Cervus Elaphus corsicanus

M. Rustici[1], G. Lai[1], A. Facchini[2] & S. Bastianoni[2]
[1]*Sassari University, Department of Chemistry, Via Vienna 2-07100, Sassari, Italy*
[2]*Siena University, Department of Chemical and Biosystems Sciences, Via della Diana 2/A 53100 Siena, Italy*

Abstract

In spite of its apparent complexity and randomness, time evolution of nonlinear dynamical systems can be often described by resorting to a low number of degrees of freedom. This is the case of mechanical apparatuses as well as of biological activities such as cell cycles and organs physiology. With reference to the latter, nonlinear phenomena and chaos have been also proven to occur in the vocal emission of living organisms as a result of both the vocal apparatus physiology and the turbulent fluid dynamics. The complexity of the vocal emissions and their apparent correlation with the social behaviours displayed make the Cervus Elaphus Corsicanus one interesting case.

The nonlinear dynamics techniques used to characterise vocalisation dynamics provide direct experimental evidence for the occurrence of chaos in the vocalising behaviour of Cervus Elaphus Corsicanus.

1 Introduction

In the well preserved evergreen forest of monte Arcosu in Sardinia (a protected area owned by WWF Italy) we can find the last remaining populations of a subspecie of the red deer: the Sardinian deer (Cervus elaphus corsicanus).

The *Cervus elaphus* is the largest and most phylogenetically advanced species of Cervus. Head and body length is 1,650-2,650 mm, tail length is 100-270 mm, height at the shoulder is 750-1,500 mm, and weight is 75-340 kg. Animals in the populations of North America and northeastern Asia are usually larger than

Paper from: *Design and Nature*, CA Brebbia, L Sucharov & P Pascola (Editors).
ISBN 1-85312-901-1

those of Europe and southern Asia, and within a given population males average larger than do females. The upper parts are usually some shade of brown, and the underparts are paler. There is a prominent pale-colored patch on the rump and buttocks. The pelage is coarse, and males have a long, dense mane. The well-developed antlers measure up to about 1,750 mm along the beam.

This deer utilizes a wide variety of habitats in both lowlands and mountains. In North America it originally was found in dense coniferous forests, open hardwood forests, chaparral, and grasslands [1]. It is usually active during the early morning and late afternoon. In some areas it moves into higher country during the spring and returns to the lowlands in the fall. Populations in eastern North America did not migrate, but those in the western mountains frequently do, the autumn movement generally being to lower elevations to avoid snow cover. Summer ranges cover a much larger area than do winter ranges. In certain areas only a portion of a population migrates. The diet of C. elaphus varies and involves both grazing and browsing. In western North America up to 85 percent of spring forage is grass, there is a shift to forbs and woody plants in the summer, browse and dried grass is taken in the fall, and shrubs and conifers extending above the snow may be used in winter [2].

In Europe and North America, mating occurs in the early fall, and births in the late spring. Females are seasonally polyestrous, the estrous cycle being about 18 days long and receptivity lasting 1-2 days. The gestation period of European red deer is about 235 days, while that of the North American elk reportedly varies from 247 to 265 days. There is usually a single offspring, which weighs 13-18 kg at birth. The calf stands quickly, follows the cow after 3 days, grazes at 4 weeks of age, and loses its spots after 3 months. Lactation may last 4-7 months, sometimes longer. Females attain sexual maturity at about 28 months and are then capable of giving birth annually. Males are capable of mating in their second year of life but usually must wait considerably longer, because of competition from older bulls. More than half of all animals die before they are 1 year old, and few wild individuals survive more than about 12-15 years; males generally perish first, because of the intensity of their fighting.

Few mammalian species have been so extensively affected by people. On the one hand, C. elaphus has been introduced to many areas beyond its natural range, and even within its natural range there has been much transplantation of populations and manipulation of herds in an effort to improve big game hunting. There now are major human-established populations in New Zealand, Australia, and Argentina. On the other hand, excessive hunting and habitat modification have resulted in drastic declines in natural distribution and numbers. There is some difficulty in assessing bioconservation status, because of the considerable disagreement regarding the division of C. elaphus into subspecies or even full species. The typical red deer, occurs in Europe, North Africa, and southwestern Asia as far east as the southern shores of the Caspian Sea. C. elaphus has disappeared from much of this region; existing populations in Europe generally are well protected, but some do not represent the original stock of the area in which they are found. There now are about 1 million red deer in Europe, the largest populations being in Scotland,

Paper from: *Design and Nature*, CA Brebbia, L Sucharov & P Pascola (Editors).
ISBN 1-85312-901-1

Germany, and Austria. The subspecies C. e. corsicanus, of Corsica and Sardinia, is classi¿ed as endangered by the IUCN and the USDI. Habitat degradation and illegal hunting reduced the number on Sardinia to about 200-400 individuals .

October is the time of year when the males round up a group of females for mating. The largest and strongest male generally has the largest harem. In order to maintain this position of superiority he must constantly see off rival males by bellowing out his echoing roar, and chasing off any which come near his females. After roaring, the larger remaining males size each other up, and if antler and body size are comparable, they battle for the females with their hardened antlers. The antlers lock and each male attempts to forcefully push the other away. The strongest and most powerful male wins and secures a harem (group) of females for mating.

Understanding the physical and physiological mechanism of sound production is important for mammal vocalization. Nonlinearities associated with the laryngeal source has been observed ([23],[24]).

In this paper we apply non linear dynamics analysis techniques to the study of sounds emitted from C. elaphus corsicanus.

2 Data analysis

A number of different signals corresponding to different sound emissions has been considered. Only clearly discernible sound emissions have been analysed, in order to focus exclusively on meaningful vocalisations avoiding any spurious effect due to echoes or noise. Fast Fourier Transform (FFT) has been used to perform preliminary analyses on vocalisation units, the presence of regions with high density of unresolved frequencies being a necessary, even if not suf¿cient, condition for the occurrence of chaotic dynamical regimes [3]. Non-linear dynamics analyses have been, therefore, limited to signal units characterised by broad-band features in the frequency domain. Results reported in the present work refer to a signal 2.157 s long. Analyses have been performed on a shorter unit extracted from the longer signal. The time series examined consists of a 7113 points and corresponds to a sound duration of 0.322 s sampled at 22050 Hz.

3 Computational methods

3.1 Attractor reconstruction

The attractor of underlying dynamics has been reconstructed in phase space by applying the time delay vector method [3, 4, 5, 6, 7]. According to this method, the system dynamical evolution is reconstructed by embedding the time series $\{x_i\}$ in a m-dimensional space. The reconstructed trajectory consists of consecutive m-dimensional vectors $y_i = (x_i, x_{i+T}, x_{i+2T}, \ldots, x_{i+(m-1)T})$, where T is some multiple integer of the sampling time. The time delay T represents a measure of correlation existing between two consecutive components of m-dimensional vec-

Paper from: *Design and Nature*, CA Brebbia, L Sucharov & P Pascola (Editors).
ISBN 1-85312-901-1

tors used in the trajectory reconstruction. Following a commonly applied methodology, the time delay T has been chosen in correspondence to the first minimum of the average mutual information function [6]. A value $T = 3$ has been obtained. A guide for the proper choice of embedding dimension m has been provided by the uniqueness theorem about the solutions of autonomous differential equations, according to which no overlap of trajectory with itself is possible neither in the original nor in the reconstructed phase space.

3.2 Lyapunov exponents

It is well known that chaotic systems display a sensitive dependence on initial conditions. Such a property deeply affects the time evolution of infinitesimally close trajectories, $\mathbf{u}(\mathbf{t})$, which tend to diverge when the system dynamics is governed by chaotic behaviours. Lyapounov exponents measure the rate of divergence. Actually, even in the case of a single dynamic variable time series, a Spectrum of Lyapounov Exponents (SLE) can be evaluated. The total number of exponents depends on the dimension of the phase space in which dynamics is embedded. In the case of a n-dimensional phase space, n Lyapounov exponents $(\lambda_1 \geq \lambda_2 \geq \ldots \geq \lambda_n)$ are defined. Each one of the n Lyapounov exponents measures then the orbital stability along a proper direction. In particular, the system behaviour will become more and more chaotic as the number of positive Lyapounov exponents increases. The largest one, λ_1, determines the degree of chaoticity and, correspondingly, the timescale on which the dynamics becomes unpredictable. Various methods have been developed to evaluate the SLE [4, 8, 9, 10, 11, 12, 13]. All of them consider the trajectory defined by the reconstructed attractor as a fiducial trajectory. SLE calculation is performed by studying trajectories originating from points nearby the fiducial trajectory, each point being considered as a distinct initial condition along the fiducial trajectory itself. The method allows, therefore, an approximate reconstruction of the unknown dynamics $\mathbf{f}$ in the neighborhood of the fiducial trajectory. In the present paper, the Brown *et al.* algorithm [5, 13], approximating the unknown dynamics by polynomials of degrees n, with $n > 1$, has been used. The number of active dynamical degrees of freedom, d_L, corresponding to the number of Lyapunov exponents, has been previously evaluated by the application of the local false nearest neighbours method [14].

When data are embedded in a m-dimensional space, the complete spectrum of exponents consists of m values. Embedding theorem states that an embedding space with a dimension about twice the one of the chaotic attractor has to be chosen. Embedding space might therefore have a larger dimension than the "true" underlying space and spurious Lyapounov exponents, not defined in the true state space, might occur in the reconstructed state space as artifacts of the reconstruction process [15]. For such a reason, it is useful to evaluate independently the maximum Lyapounov exponent. The algorithm recently proposed by Rosenstein and Kantz [16, 17], fast and robust to changes in quantities such as embedding dimension, size of data set, reconstruction delay and noise level, has been applied by taking advantage of the sub-routine `Lyap_r` contained in the software package TISEAN

Paper from: *Design and Nature*, CA Brebbia, L Sucharov & P Pascola (Editors).
ISBN 1-85312-901-1

[18, 19, 20].

4 Results and Discussion

Signal considered is characterised by highly complex patterns in which different transients with both periodic and apparently aperiodic features can be identified. Part of the examined vocalisation unit is reported in Fig. 1. The apparently random behaviour of the numerical series, easily detectable with a simple visual inspection of the sound pattern, has been confirmed by the amplitude spectrum reported in Fig. 2. Three different regions can be put into evidence. At low frequencies, between 0 and 70 Hz, a first distribution of unresolved peaks is present. A sharp peak is also present at 450 Hz, while a broad band of frequencies, ranging between 850 and 950 Hz, is easily recognisable.

The false nearest neighbours method [7] has provided an embedding dimension $m = 6$. A three-dimensional projection of a 1000 points long portion of the reconstructed attractor is shown in Fig. 3. It is worth noting that, in spite of the apparent randomness of the vocal emission signal, the attractor structured qualities suggest an underlying deterministic dynamical evolution.

In order to carefully characterise the nature of vocalisation dynamics, the spectrum of Lyapunov exponents has been evaluated. Average values of Lyapunov exponents have been reported in Fig. 4 as a function of the number of steps forward L [5, 13, 14]. Values are reported in units inverse of the sampling time $T_S = 4.535 \times 10^{-5}$ s. Each point has been obtained by following and averaging the behaviour of two nearby trajectories for L steps of the sampling time forward over 3000 initial locations on the attractor.

Owing to the lack of information on the dynamical operator mapping the reconstructed attractor, the evaluation of the six Lyapunov exponents from the experimental time series has required an approximate reconstruction of the unknown dynamics. The number of dynamical degrees of freedom active, d_L, corresponding to the number of Lyapunov exponents, has been previously evaluated by the application of the local false nearest neighbours method [14]. A value $d_L = 6$ has been found (Fig. 3). The occurrence of a positive Lyapunov exponent points out the chaotic nature of the vocalisation behaviour investigated. The Kaplan-Yorke fractal dimension D_L of the attractor [21], equal to $D_L = 2.58$, confirms the high dimensional fractal qualities of the strange attractor. Chaoticity is also confirmed by the measure of the maximum Lyapounov exponent. The value of $< \ln d_j(i) >$ is reported in fig. 5 as a function of the time $i\Delta T$ for different values of the embedding dimension ($m = 10, 12, 14, 18, 20$). Derivatives are reported in Fig 6. A saturation region is present in the range $200 \leq t \leq 300$ where slopes are constant for different m values. In other words, a set of approximately parallel lines has been obtained, each one with a slope roughly proportional to λ_1. The largest Lyapounov exponent, equal to $\lambda_1 = 372.8 \pm 2.6 \cdot 10^{-5}$, has been accurately evaluated by using a least-squares fit to the average line. Although numerical agreement between the λ_1 evaluated with Rosenstein [16] (Fig. 6) alghoritm and those evaluate with Bryant [13, 5] method, is not observed, the chaotic nature of the temporal

Paper from: *Design and Nature*, CA Brebbia, L Sucharov & P Pascola (Editors).
ISBN 1-85312-901-1

series studied is confirmed. Such a result has been further corroborated by the analysis of a randomised temporal series, which do not present any linear region. The behavior is instead similar to those obtained from random series. This result indirectly confirms the chaotic and deterministic nature of the signal analysed.

5 Concluding remarks

In this paper we put in evidence the nonlinear chaotic behaviour of the vocalization of Cervus Elaphus Corsicanus. The analysis methods are quite robust and well supported by a large amount of literature. This result is another proof of the strong nonlinearities that a mammalian vocal apparatus can exhibit and can be useful in the identification of the characteristic parameters of the two mass model of the mammalian larynx [22].

References

[1] Skovlin, J. M. 1982. Habitat requirements and evaluations. In Thomas and Toweill (1982), pp. 369-413.
[2] Nelson, J. R., and T. A. Leege. 1982. Nutritional requirements and food habits. In Thomas and Toweill (1982), pp. 323-67.
[3] E. Ott, *Chaos in dynamical systems* (Cambridge University Press, New York, 1993).
[4] J. P. Eckmann and D. Ruelle, Rev. Mod. Phys. **57**, 617 (1985).
[5] H. D. I. Abarbanel, *Analysis of observed chaotic data* (Springer-Verlag, New York, 1996).
[6] A. M. Fraser and H. L. Swinney Phys. Rev. A **33**, 1134 (1986).
[7] M. B. Kennel, R. Brown, and H. D. I. Abarbanel, Phys. Rev. A **45**, 3403 (1992).
[8] J. M. Greene and J. S. Kim, Physica D, **13**, 261 (1987).
[9] J. P. Ekmann, S. O. Kamphorst, D. Ruelle and S. Ciliberto, Phys. Rev. A, **34**, 4971 (1986).
[10] A. Wolf, J. B. Swift, H. L. Swinney, and J. A. Vastano, Physica **16D**, 285 (1985).
[11] M. Sano and Y. Sawada, Phys. Rev. Lett., **55**, 1082 (1985).
[12] P. Bryant and R. Brown, Phys. Rev. Lett., **65**, 1523 (1990).
[13] P. Bryant, R. Brown and H. D. I. Abarbanel, Phys. Rev. A, **43**, 2787 (1991).
[14] H. D. I. Abarbanel and M. B. Kennel, Phys. Rev. E **47**, 3057 (1993).
[15] T. D. Sauer, J. A. Tempkin and J. A. Yorke, Phys- Rev. Lett. **81**, 4341 (1998).
[16] M. T. Rosenstein, J. J. Collins and C. J. De Luca, Physica D **65**, 117 (1993).
[17] H. Kantz, Phys. Lett. A **185** 77.
[18] H. Kantz and T. Schreiber, in *Nonlinear Time Series Analysis* (Cambridge University Press 1997).
[19] The TISEAN software package is publicy available at http://www.mpipks-dresden.mpg.de/~tisean/TISEAN_2.1/index.html. The distribution includes

Paper from: *Design and Nature*, CA Brebbia, L Sucharov & P Pascola (Editors).
ISBN 1-85312-901-1

an online documentation system.
[20] R. Hegger, H. Kantz and T. Schreiber, CHAOS, **9**, 413 (1999).
[21] J. Kaplan and J. A. Yorke, Springer lecture notes in mathematics **730**, 204 (1979).
[22] H. Herzel, D. Berry, I. Titze and I. Steincke, Nonlinear dynamics of the voice: Signal analysis and biomechanical modeling, *CHAOS 5(1)*, 1995.
[23] M. S. Fee, B. Sharaiman, B. Pesaran and P. P. Mitra 1998 The role of nonlinear dynamics of the syrinx in the vocalizations of a songbird *Nature 395 67-71.*
[24] I. Wilden, H. Herzel, G. Peters and G. Tembrock 1998 Subharmonics, biphonation and deterministic chaos in mammal vocalization Bioacoustics 9 171-196.
[25] P. Mergell, W. Fitch and H. Herzel, Modeling the role of nonhuman vocal membranes in phonation, *J. Acoustical Soc. of America* **105**(3), march 1999 2020-2028.
[26] I. Steinecke, H. Herzel, Bifurcations in an asymmetric vocal fold model, *J. Acoustical Soc. of America* **97***(3), march 1995 1874-1884.*

www.witpress.com witpress@witpress.com
ISBN 1-85312-901-1

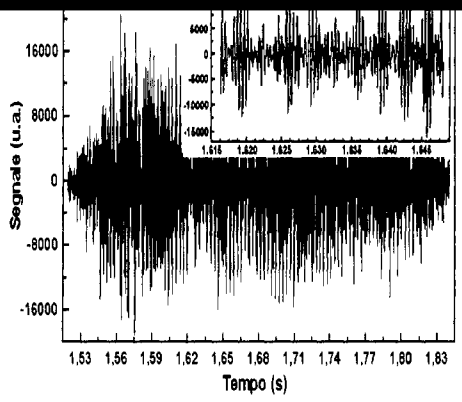

Figure 1: A small portion of the analyzed signal unit. An enlarged picture has been reported in the inset for the sake of clarity. An apparent random variation is superposed to a regular modulation of the signal.

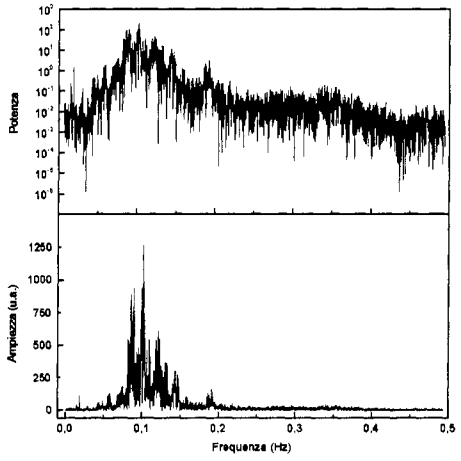

Figure 2: The amplitude spectrum of the analysed time series.

Paper from: *Design and Nature*, CA Brebbia, L Sucharov & P Pascola (Editors).
ISBN 1-85312-901-1

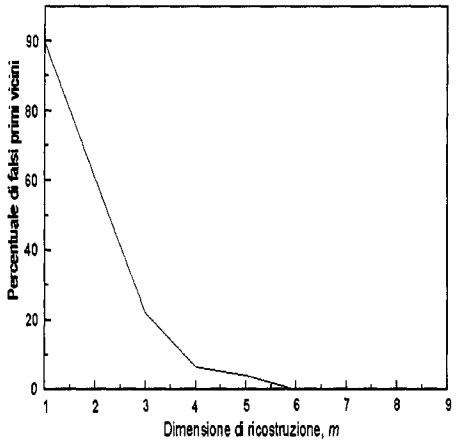

Figure 3: The embedding dimension calculated by false nearest method (`false-nearest` routine in TISEAN package).

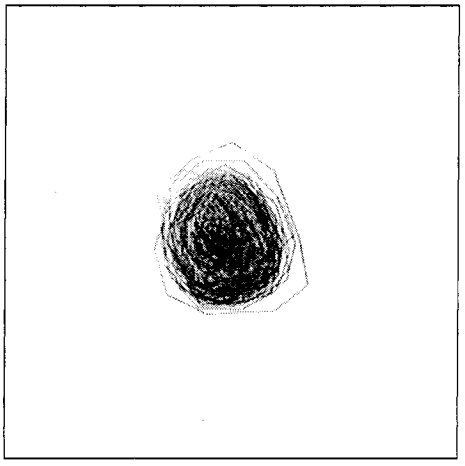

Figure 4: A three-dimensional projection of the time delay method reconstructed attractor (`delay` routine). A 200 point long portion of the reconstructed attractor has been reported for sake of clarity.

Paper from: *Design and Nature*, CA Brebbia, L Sucharov & P Pascola (Editors).
ISBN 1-85312-901-1

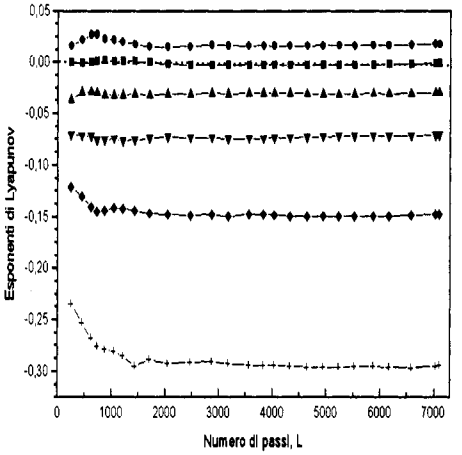

Figure 5: The average Lyapunov exponents as a function of the number of steps L forward each location (`Lyap-spec` routine). The values are reported in units inverse of the sampling time $T_S = 4.535 \times 10^{-5}$ s.

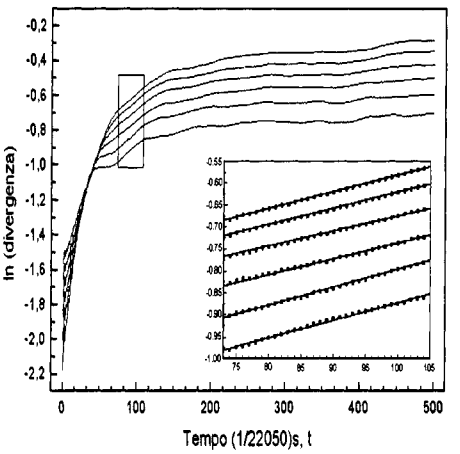

Figure 6: The maximal Lyapunov exponent, calculated by rosenstein (`lyap-r routine`) algorithm.